

Article

Development of a New Finishing Process Combining a Fixed Abrasive Polishing with Magnetic Abrasive Finishing Process

Yanhua Zou ^{1,*}, Ryunosuke Satou ¹, Ozora Yamazaki ² and Huijun Xie ³

¹ School of Engineering, Course of Mechanical Engineering Systems, Utsunomiya University, 7-1-2 Yoto, Utsunomiya, Tochigi 321-8585, Japan; satoryu@cc.utsunomiya-u.ac.jp

² Graduate School of Regional Development and Creativity, Utsunomiya University, 7-1-2 Yoto, Utsunomiya, Tochigi 321-8585, Japan; mc196754@cc.utsunomiya-u.ac.jp

³ Graduate School of Engineering, Utsunomiya University, 7-1-2 Yoto, Utsunomiya, Tochigi 321-8585, Japan; dt187109@cc.utsunomiya-u.ac.jp

* Correspondence: yanhua@utsunomiya-u.ac.jp; Tel.: +81-28-689-6057

Abstract: High quality, highly efficient finishing processes are required for finishing difficult-to-machine materials. Magnetic abrasive finishing (MAF) process is a finishing method that can obtain a high accuracy surface using fine magnetic particles and abrasive particles, but has poor finishing efficiency. On the contrary, fixed abrasive polishing (FAP) is a polishing process can obtain high material removal efficiency but often cannot provide a high-quality surface at the nano-scale. Therefore, this work proposes a new finishing process, which combines the magnetic abrasive finishing process and the fixed abrasive polishing process (MAF-FAP). To verify the proposed methodology, a finishing device was developed and finishing experiments on alumina ceramic plates were performed. Furthermore, the mechanism of the MAF-FAP process was investigated. In addition, the influence of process parameters on finishing characteristics is discussed. According to the experimental results, this process can achieve high-efficiency finishing of brittle hard materials (alumina ceramics) and can obtain nano-scale surfaces. The surface roughness of the alumina ceramic plate is improved from 202.11 nm *Ra* to 3.67 nm *Ra* within 30 min.

Keywords: fixed abrasive; magnetic abrasive finishing; alumina ceramic; surface finishing; brittle hard materials



Citation: Zou, Y.; Satou, R.; Yamazaki, O.; Xie, H. Development of a New Finishing Process Combining a Fixed Abrasive Polishing with Magnetic Abrasive Finishing Process. *Machines* **2021**, *9*, 81. <https://doi.org/10.3390/machines9040081>

Academic Editor: Mariusz Deja

Received: 17 March 2021

Accepted: 9 April 2021

Published: 12 April 2021

Publisher's Note: MDPI stays neutral with regard to jurisdictional claims in published maps and institutional affiliations.



Copyright: © 2021 by the authors. Licensee MDPI, Basel, Switzerland. This article is an open access article distributed under the terms and conditions of the Creative Commons Attribution (CC BY) license (<https://creativecommons.org/licenses/by/4.0/>).

1. Introduction

Magnetic abrasive finishing (MAF) process are used for the precision finishing of the inner surface of circular tubes, the mirror finishing of flat parts, and the precision edge finishing of complex curved parts [1–3]. Among them, when using the plane MAF process, a certain gap is provided between the magnetic pole and the workpiece, and a magnetic brush composed of fine particles (mixed magnetic particles and abrasive particles) is formed in this gap. Although this process can obtain a better surface finish, there is a problem in material removal efficiency, and there is a strong demand for improving the finishing efficiency. Shinmura et al. [4,5] proposed and designed a plane MAF device, which generates a magnetic field from an electromagnet. The process principle of plane MAF is analyzed, and the influence of the supply weight of finishing fluid and magnetic abrasive on the grinding depth and surface roughness is discussed. In references [6,7], they also discussed the finishing of the outer surface of the cylinder and the inner surface of the tube through the MAF process, and investigated the influence of some process parameters on the finishing characteristics. Zou et al. [8–10] proposed the MAF process using an alternating magnetic field. They investigated the process mechanism and finishing characteristics, and concluded that the MAF process using an alternating magnetic field can achieve higher finishing efficiency and surface quality compared with the case of a static magnetic field. Wang et al. [11] discussed the use of MAF process for finishing pipes

of three materials, such as Ly12 aluminum alloy, 316L stainless steel and H62 brass. They reported that using transformer oil or stearic acid liquid can significantly improve material removal rate (MRR), because transformer oil helps to form a physisorption film, and stearic acid helps to form a chemisorption film. Jiao et al. [12] applied the MAF process to improve the surface quality of the hole wall and eliminate burrs on the edge of the hole. They used 7075 aluminum alloy as a workpiece, and analyzed the influence of magnet spinning speed, abrasive mesh, and abrasive filling amount on the diameter deviation of the hole and surface roughness of the inner wall. They reported that the burrs were significantly removed and the burr removal efficiency was improved by 33.3% compared with the conventional magnetic abrasive finishing process. Vahdati et al. [13] applied the MAF process to finishing aluminum pipes. They discussed the influence of the magnetic flux density, machining time, the amount of magnetic abrasive powder and the rotation speed of the workpiece on the surface roughness. According to the experimental results, using permanent magnets of 1 T, the amount of 8 g of ilmenite powder of mesh 150, rotating speed of 750 rpm, and 30–40 min of process time, will result into a surface roughness of 0.45 μm R_a from the original value of 2 μm R_a . Gheisari et al. [14] proposed a new machining process to use magnetorheological (MR) fluid to finish the cylindrical surface. They showed that the application of fast rectilinear alternating motion in the process can effectively improve the surface of the workpiece, and the surface roughness of the aluminum cylinder can be improved from about 200 nm R_a to 50 nm R_a . Yin et al. [15,16] improved the deburring efficiency of edges by using the vibration-assisted MAF process. They proposed a method for polishing 3D micro-curved surfaces using vibration-assisted MAF technology, and studied the effects of three vibration modes (horizontal vibration, vertical vibration, and compound vibration) on magnetic field, polishing pressure, abrasive behavior, and polishing performance. Lin et al. [17] polished the free-form surface through the MAF process. The Taguchi experimental design was used to investigate the effects of magnetic field, spindle speed, feed speed, working gap, abrasives, and lubricants. After two-stage finishing, the surface roughness R_{max} is improved from 2.670 μm to 0.102 μm . Guo et al. [18] proposed a localized vibration-assisted magnetic abrasive polishing (VAMAP) method for the finishing of V-grooves and Fresnel optical elements. They showed that this method can improve the surface roughness of the workpiece from an initial value of more than 10 nm R_a to about 7 nm R_a while the microfeatures of V-groove and Fresnel optics were well maintained.

On the contrary, the fixed abrasive polishing (FAP) process has a higher material removal efficiency than the free abrasive polishing process [19–21]. Therefore, it can be used to polish hard brittle materials, such as silicon wafers, glass, and ceramics [22–24]. However, the FAP process is inferior to the free abrasive polishing process and the MAF process in terms of surface finish. Luo et al. [25] investigated the use of semi-fixed and fixed polishing film with diamond and alumina abrasive for the polishing of SiC and sapphire substrates. They concluded that when the material removal scale is tens of nanometers or more, the removal mode of the substrate is brittle removal. When the material removal scale is nanoscale, it is a plastic removal mode. They also discussed the material removal mechanism of semi-fixed and fixed diamond abrasive polishing tools for processing SiC substrates. They concluded that massive scratches and pits were generated due to the unequal protrusion height of the diamond grits in the fixed polishing film. However, in the semi-fixed abrasive polishing, due to the retraction during the polishing process, the protrusion height of the diamond grits is basically the same, which makes it easier to obtain smooth and scratch-free substrate surface with nanoscale roughness [26]. Huang et al. [27] discussed the processing characteristics and mechanism of GO/SiO₂ nano-slurry in a fixed abrasive process. They showed that grinding with GO/SiO₂ slurry can reduce the surface damage to the glass and achieve a crack-free subsurface. In comparison with traditional grinding, this process reduces the surface roughness by 35% and the material removal rate increases by 28%. Zhou et al. [28] investigated the mechanical removal behavior of SiC substrates during polishing with fixed abrasives by molecular dynamics simulation. They

showed that the random distribution of diamond abrasives will reduce the processing quality, and optimizing the arrangement and exposed height of the abrasives in the fixed abrasive pad will help improve the processing quality. Cho et al. [29] investigated the mechanism of material removal when polishing glass substrates (borofloat, BK7, and quartz) by fixed abrasive grinding. They show that the material removal of the glass substrate follows the brittle fracture model. Jiao et al. [30] proposed the ultrasonic-assisted fixed-abrasive lapping (UAFL) technology, and conducted theoretical and experimental studies on the mechanism and characteristics of UAFL. The results show that the superimposed ultrasonic vibration helps to improve the material removal rate and surface quality.

In recent years, the widespread use of hard and brittle materials such as titanium alloys, glass, and ceramics has promoted the development of corresponding surface finishing processes. Although the MAF process has better surface quality after finishing, its finishing efficiency is lower than that of FAP process. Therefore, we propose a new finishing process, magnetic abrasive finishing process combined with the fixed abrasive polishing process (MAF-FAP), and expect it to achieve high-efficiency finishing of brittle hard materials and achieve nano-scale surface quality. In this paper, we discussed the finishing mechanism of MAF-FAP process. The difference in finishing efficiency and surface quality between this process and FAP process was investigated when finishing alumina ceramic plates. In addition, the influence of different process parameters on finishing characteristics is discussed.

2. Processing Principle and Experimental Setup

2.1. Processing Principle

Figure 1 shows the processing principle of the conventional plane MAF process. The basic principle of the conventional plane MAF process is to fill the magnetic abrasive or compound magnetic finishing fluid between the magnetic pole and the workpiece. Magnetic abrasives are made of iron powder and abrasives through sintering or chemical or other techniques [31]. However, sintering requires both high temperature and pressure within an inert gas atmosphere. Subsequently, the sintered material should be crushed mechanically and then sieving is required to sort it into a specific particle size. Obviously, due to the complex production process, additional production costs will increase [32]. Therefore, more and more researches have focused on the use of unbound magnetic abrasives [33–35]. The compound magnetic finishing fluid is obtained by uniformly mixing a certain proportion of magnetic particles, abrasive particles, and grinding fluid. In the magnetic field, the magnetic particles are attracted by the magnetic poles and arranged along the lines of magnetic force to form a magnetic brush. The relative movement between the magnetic brush and the workpiece is generated through the feed movement and the rotation movement, thereby realizing the material removal on the surface of the workpiece. However, since the tangential force and normal force of the MAF process are mainly limited by the magnetic force, the finishing efficiency is lower than that of the FAP process. In order to improve the finishing efficiency and realize the ultra-precision surface finishing, a new finishing process is proposed which combines FAP process and the MAF process.

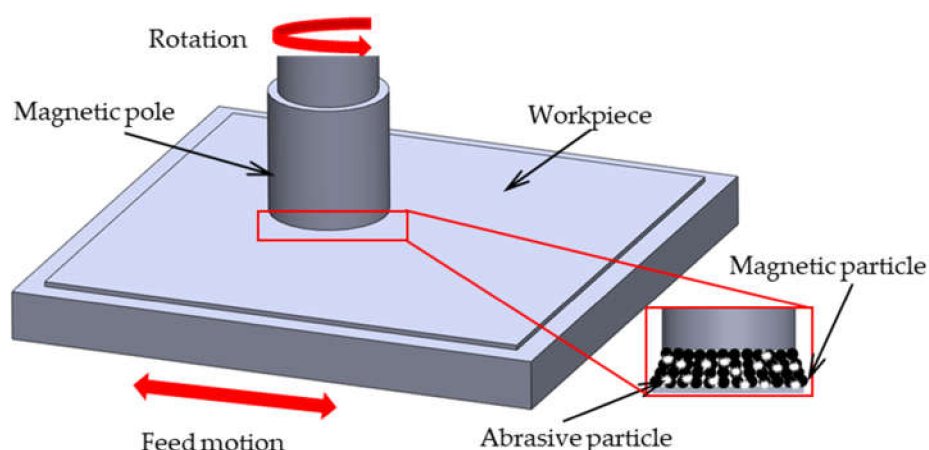


Figure 1. Processing principle of the conventional plane MAF process.

A schematic diagram of MAF-FAP process is shown in Figure 2. Here magnetic particles are adsorbed to the combined tool surface by magnets attached to the FAP tool, and by applying a grinding liquid with abrasive particles onto the surface of the workpiece, a magnetic brush with abrasive particles is formed. A slide table is attached to the lower part of the workpiece, and the workpiece is reciprocated left and right to realize the feed movement. At the same time, constant pressure is applied to the combined tool to make the normal load constant during the finishing process. In addition, the combined tool can perform the rotational movement. Therefore, in the finishing process, the combined tool acts on the workpiece with constant pressure, and at the same time, the combined tool performs rotational movement and horizontal feed movement relative to the workpiece. As a result, the fixed abrasive on the surface of the FAP tool and the abrasive particles absorbed into the magnetic brush act on the surface of the workpiece in a combined manner to achieve finishing of the workpiece surface.

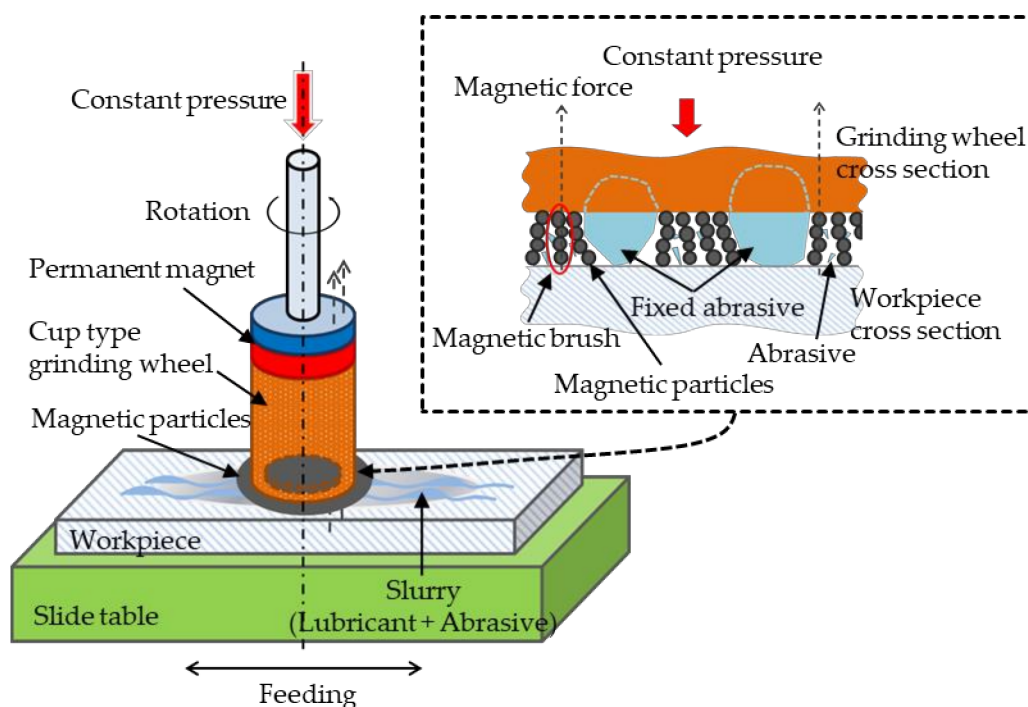


Figure 2. Processing principle of the MAF-FAP.

2.2. Experimental Setup

Figure 3 shows an external view of the experimental device. The experimental device was modified by a desktop drilling machine NS-14R (manufactured by Nakane, Tokyo, Japan), where a pulley was connected to the lever part that lowers the chuck, and weight can be attached to the pulley to apply arbitrary load on the workpiece. The combined tool is connected to the main shaft of the drilling machine through a chuck and realizes a rotational movement. In the finishing process, the normal load acting on the workpiece is measured by the load cell under the workpiece table. The horizontal feed movement of the workpiece is provided by an electric linear slides. In addition, the sliding table is fixed on an X-Y table, and the processing area can be adjusted manually.

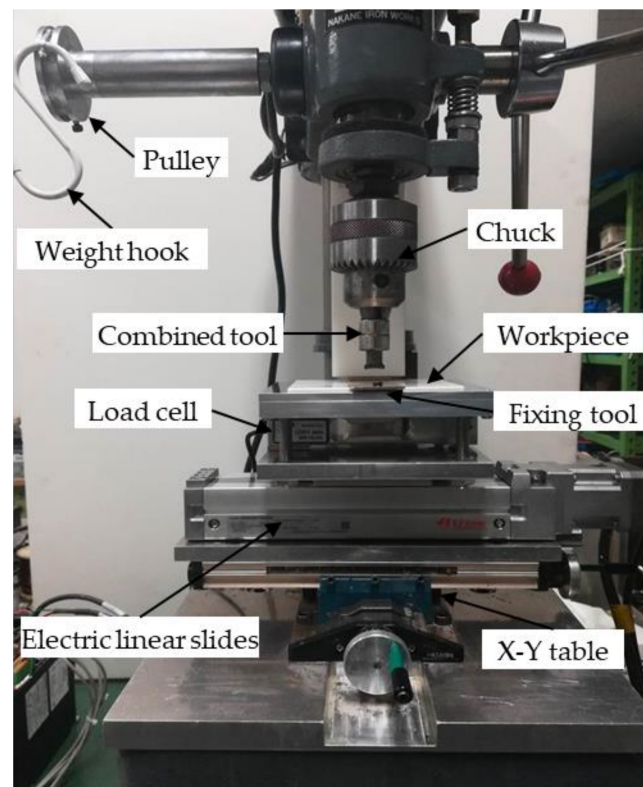


Figure 3. External view of the experimental setup.

Figure 4 shows the external view of the combined tool. The combined tool is composed of a fixed abrasive tool (cup-type electrodeposition diamond wheel) and two permanent magnets. The grinding surface of the fixed abrasive tool has an outer diameter of 10 mm and an inner diameter of 8 mm. The magnetic field is provided by two ring-shaped permanent magnets with an inner diameter of 6.5 mm, an outer diameter of 19 mm, and a thickness of 10 mm. The magnetic particles are attracted to the bottom surface of the grinding wheel to form a magnetic brush. The combination of magnetic brush and grinding wheel constitutes the grinding tool for this process.



Figure 4. External view of combined tool.

The normal load adjustment system is shown in Figure 5. The combined tool can move in a certain range in the vertical direction. The combined tool is applied with a normal load, which presses the workpiece. There is a load cell (LCB-03, produced by A&D CO., LTD., Tokyo, Japan) under the workpiece, which can measure the load from 0 to 100 N. The load cell is connected to the Digital indicator (AD-4532B, produced by A&D CO., LTD., Tokyo, Japan), and the load value is obtained through the logger (midi LOGGER GL240 produced by Graphtec Corporation, Yokohama, Japan). According to the difference between the load value obtained by the logger and the expected load value, increase, or decrease the normal load applied to the combined tool.

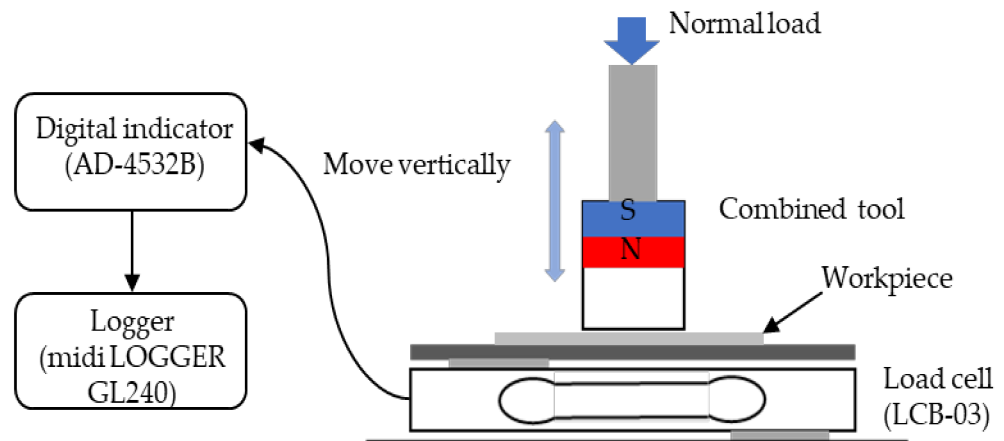


Figure 5. Normal load adjustment system.

2.3. Force Analysis

Figure 6 shows a schematic diagram of the force analysis of MAF-FAP. The magnetic particles are concentrated and adsorbed in the finishing zone by receiving the magnetic forces ΔF_x and ΔF_y (the resultant force ΔF) expressed by the following equations from the magnetic pole in the direction of the magnetic force line (x -axis direction) and the direction of the equipotential line (y -axis direction) [36].

$$\Delta F_x = V_0 \chi \mu_0 H \left(\frac{\partial H}{\partial x} \right), \quad (1)$$

$$\Delta F_y = V_0 \chi \mu_0 H \left(\frac{\partial H}{\partial y} \right), \quad (2)$$

where V_0 is the volume of the magnetic particles, χ is susceptibility of the magnetic particles, μ_0 is permeability of vacuum, H is the magnetic field intensity, $(\partial H/\partial x)$ and $(\partial H/\partial y)$ are the rate of change of the magnetic field in the x and y coordinate directions, respectively, and x and y are the coordinates. Equations (1) and (2) indicate that the magnitude of the

magnetic force acting on the magnetic particles increases as the volume of the magnetic particles increases.

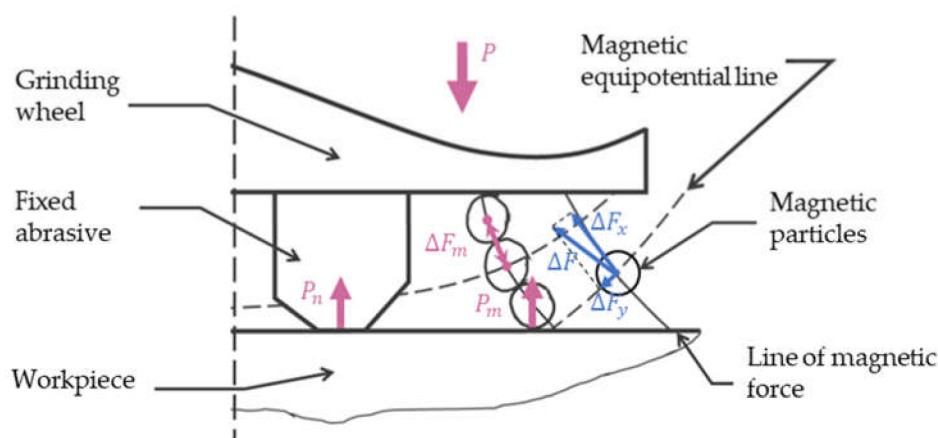


Figure 6. Schematic diagram of force analysis.

Further, assuming a spherical particle shape, the magnetic attraction force ΔF_m between magnetic particles can be calculated as [37]

$$\Delta F_m = \frac{3\pi r^2 \mu_0 \chi_r^2 H^2}{2(3 + \chi_r)^2}, \quad (3)$$

where r is the radius of each magnetic particle and χ_r is the specific magnetic susceptibility of each magnetic particle. Thus, Equation (3) suggests that the larger the particle size of the magnetic particles, the stronger the adsorption between the particles. Therefore, if the diameter of the magnetic particles is large, it is considered that the formed brush shape can be maintained easily.

The combined tool that receives the pressure P distributes the pressure to the fixed abrasive particles and the magnetic brush. At this time, the relationship between normal load P applied to the combined tool and the polishing pressures P_n and P_m applied to the workpiece is given by the equation

$$P = nP_n + mP_m, \quad (4)$$

where n and m are the number of fixed abrasive particles and magnetic brushes acting on the workpiece, respectively, and P_n and P_m represent the polishing pressure exerted on the workpiece by the fixed abrasive particles and by the magnetic brush, respectively.

Qualitatively, P_m increases as ΔF_m increases. Therefore, when the pressure (P) is constant, when the diameter of the magnetic particles is large, the polishing pressure (P_m) given by the magnetic brush increases, and the polishing pressure (P_n) of the abrasive particles decreases. This will inevitably lead to different effects on the finishing characteristics when using different sizes of magnetic particles and different normal loads, which will be discussed in detail in the experimental chapter.

3. Experimental Conditions and Method

To investigate the performance and mechanism of the combined tool, the magnetic particle diameter and the load were changed, and the finishing experiment of alumina ceramic plate was performed. Table 1 shows the experimental conditions. The grinding liquid and abrasive particles are thoroughly mixed and used as a slurry. About 2 mL was applied to the polishing area first to avoid drying of the polishing surface and another ~1 mL was applied after 5 min. The surface roughness of the workpiece is measured by the surface roughness meter (SURFPAK-SV produced by Mitutoyo Corporation, Kawasaki, Japan). The evaluation standard of surface roughness uses arithmetic average roughness

(*Ra*). Before finishing, select three points to measure on the workpiece, and the average of the three measurements is taken as the initial surface roughness. The initial surface roughness of the workpiece is 140 nm to 210 nm, with an average of about 171 nm. In subsequent measurement, the measurement position is the same as the selected 3 points before finishing, and the average of the three measurement results is taken as the surface roughness. First, the finishing characteristics of the MAF-FAP process and FAP process were compared. Secondly, the influence of different normal loads on the finishing characteristics when the average diameter of the magnetic particles is 75 μm and 330 μm is discussed.

Table 1. Experimental conditions.

Parameters	Conditions
Workpiece	Alumina ceramic plate (SSA-S) ($100 \times 100 \times 2.5 \text{ mm}^3$)
Fixed abrasive tool	Cup-type electrodeposition diamond wheel # 120 (KURE GRINDING WHEEL SDEM21) Grinding surface: Outer diameter 10 mm \times Inner diameter 8 mm)
Grinding fluid	Water insoluble polishing oil (Castrol Honailo 988): 3 mL
Abrasive	Diamond abrasive (2–4 μm) (TOMEI CARAT: 50): 0.15 g
Permanent magnet	Nd–Fe–B ring permanent magnet \times 2 (Outer diameter 19 mm \times Inner diameter 6.5 mm \times 10 mm)
Magnetic particles	Electrolytic iron powder, 75 μm in mean dia: 0.15 g Electrolytic iron powder, 330 μm in mean dia: 0.15 g
Rotational speed	560 rpm
Feeding speed	2 mm/s
Load	1 N, 3 N, 10 N, 30 N
Finishing time	10 min \times 3
Surface roughness before finishing	<i>Ra</i> : 0.171 μm (0.140–0.210 μm)

When using a new FAP tool, due to the difference of some factors (such as the height of the fixed abrasive protrusion), this will have an impact on the accurate evaluation of the finishing effect. Therefore, the new FAP tool was pretreated under the same conditions, as shown in Figure 7. The conditions of the pretreatment process are shown in Table 2. The tool used in the pretreatment process is a fixed abrasive diamond pellet. The normal load is set to 4 N, and the rotational speed is set to 1800 rpm. The pretreatment time is 10 min.



Figure 7. Pretreatment of fixed abrasive tool.

Table 2. Pretreatment conditions.

Parameters	Conditions
Pretreatment tool	Fixed abrasive diamond pellet
Grinding fluid	Water insoluble polishing oil (Castrol Honailo 988): 3 mL
Rotational speed	1800 rpm
Feeding speed	0.01 mm/s
Load	4 N
Finishing time	10 min

4. Experimental Results and Discussion

4.1. Comparison of FAP and MAF-FAP

This experiment compares the finishing characteristics of the FAP process and the MAF-FAP process. In the MAF-FAP process, magnetic particles with an average diameter of 75 μm and 330 μm are used respectively. The total normal load is set to 10 N. The change of surface roughness with time is shown in Figure 8, and it can be seen that the surface roughness is improved only when magnetic particles with an average diameter of 330 μm are used. In the case of the FAP process, the surface roughness increases most obviously, followed by the case where the average diameter of the magnetic particles is 75 μm . Figure 9 shows the material removal rate (MRR) in the three cases. Corresponding to the change in surface roughness, the highest MRR in the case of FAP is obtained. In the case of MAF-FAP, MRR is much smaller than FAP, and when the magnetic particle size is 75 μm , the MRR is higher than when the magnetic particle size is 330 μm . In the case of FAP, since there is no magnetic brush to share the normal load, the depth of the fixed abrasive particles entering the workpiece increases, which leads to brittle fracture. Therefore, the amount of material removed is greater and the surface roughness increases. According to the force analysis of the MAF-FAP process, the magnetic attraction force between the magnetic particles increases with the increase of the volume of the magnetic particles (Equation (3)), and at the same time increases with the increase of the magnetic field intensity. Since the magnetic field decreases as the distance from the magnetic pole increases, the ability of the magnetic brush to maintain its shape increases as the volume of the magnetic particles increases and the distance from the magnetic pole decreases. When the average diameter of the magnetic particles is 75 μm , the shape retention capacity of the magnetic brush is lower than 330 μm . This will result in a different distribution of normal loads. In the case where the average diameter of the magnetic particles is 330 μm , P_m increases due to the increase in the magnetic attraction force between the magnetic particles. In turn, the normal load acting on the fixed abrasive particles is reduced, which reduces the depth of the fixed abrasive particles into the workpiece. Although this reduces MRR, it improves surface quality.

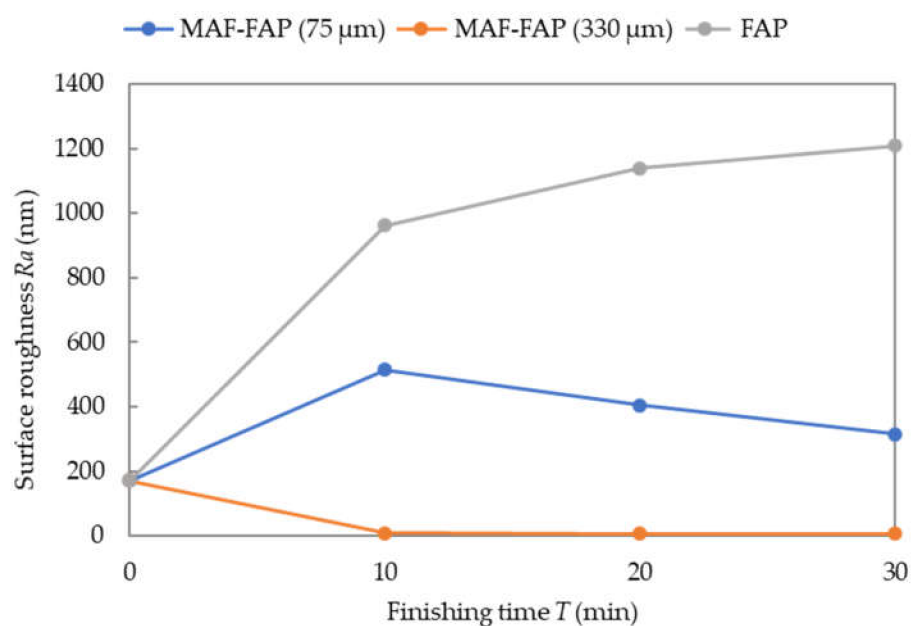


Figure 8. Change of surface roughness with time (Load: 10 N).

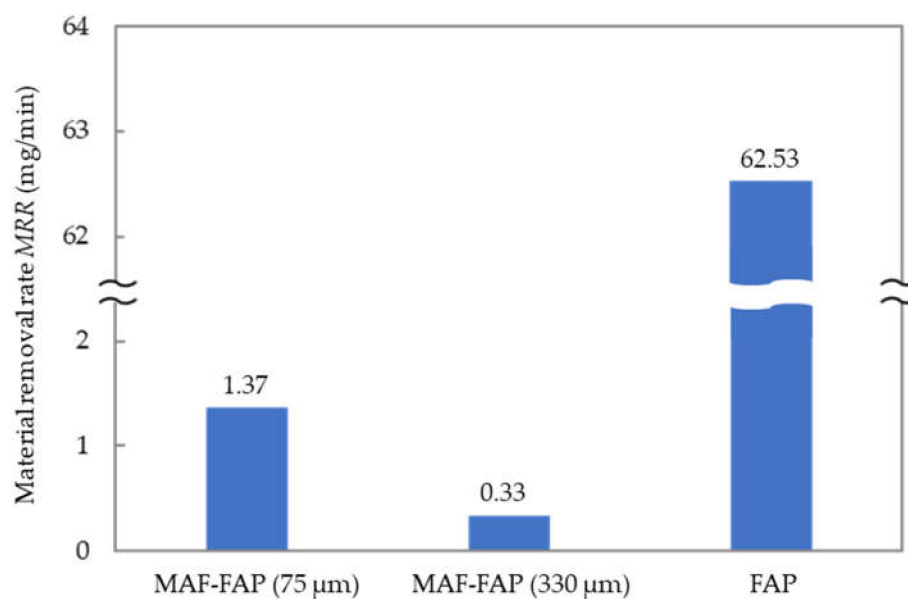


Figure 9. Material removal rate (Load: 10 N).

According to the experimental results, it can be found that when the normal load is 10 N and the average diameter of the magnetic particles is 75 μm , it is not suitable to improve the surface quality of the workpiece. Therefore, further research experiments have been carried out for these two sizes of magnetic particles.

4.2. Normal Load

In these two sets of experiments, we have investigated the influence of different normal loads on the material removal and surface roughness when the average diameter of the magnetic particles is 75 μm and 330 μm , respectively. According to the previous experimental results, when the normal load is 10 N, the average diameter of the magnetic particles is 75 μm , and the surface roughness is increased. Therefore, in this set of experiments, the normal load is set to 1 N, 3 N, and 10 N. When the average diameter of the magnetic particles is 330 μm , the surface roughness is improved. Therefore, in order to

explore the best conditions, the cases of greater than 10 N (30 N) and less than 10 N (3 N) were investigated respectively.

Figure 10 shows the effect of normal load on material removal and surface roughness when the average diameter of magnetic particles is 75 μm . It can be seen from Figure 10 that the surface roughness increases in the case of 3 N and 10 N, and with the increase of the normal load, the increase of the surface roughness is greater. In the case of 1 N, the surface quality is improved. The amount of material removal increases with the increase of the normal load. As in the previous analysis, the force between magnetic particles (ΔF_m) limits the magnitude of the normal load (P_m) it can share. When the fixed abrasive shares too much normal load, it enters the surface of the workpiece deeper, and at the same time, the fixed abrasive particles has a larger particle size. Therefore, although the amount of material removed has increased, the surface roughness has increased.

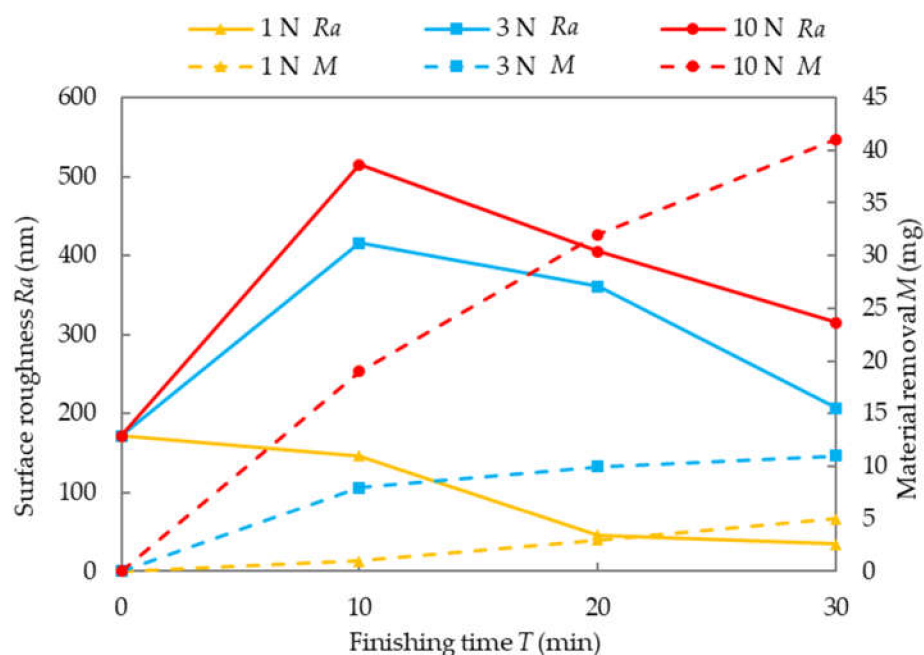


Figure 10. Effect of normal load on surface roughness and material removal (magnetic particles: 75 μm).

Figure 11 shows the effect of normal load on material removal and surface roughness when the average diameter of magnetic particles is 330 μm . It can be seen from the figure that the amount of material removal increases with the increase of the normal load, and the surface quality is also improved. However, the change rate of surface roughness is the smallest at 3 N, and is almost the same at 10 N and 30 N. Figure 12 shows the measurement results of the optical surface profiler Newview7300 (Zygo Corporation, Middlefield, OH, USA). It can be seen from the figure that the surface quality is greatly improved after finishing. According to the measurement results, when the average diameter of the magnetic particles is 330 μm and the normal load is 30 N, the surface roughness of the workpiece is improved from 202.11 nm to 3.67 nm within 30 min.

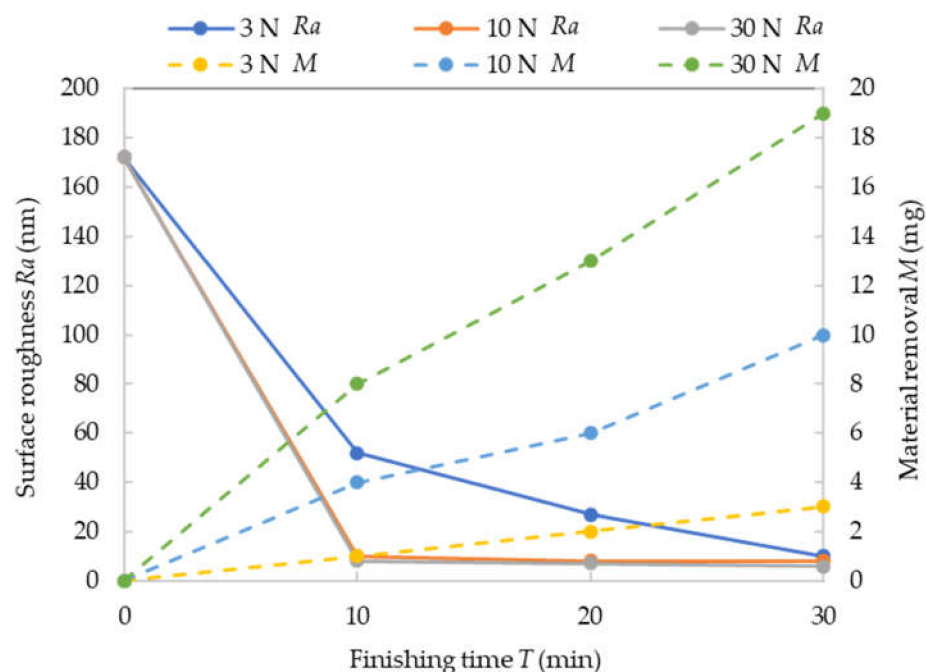


Figure 11. Effect of normal load on surface roughness and material removal (magnetic particles: 330 μm).

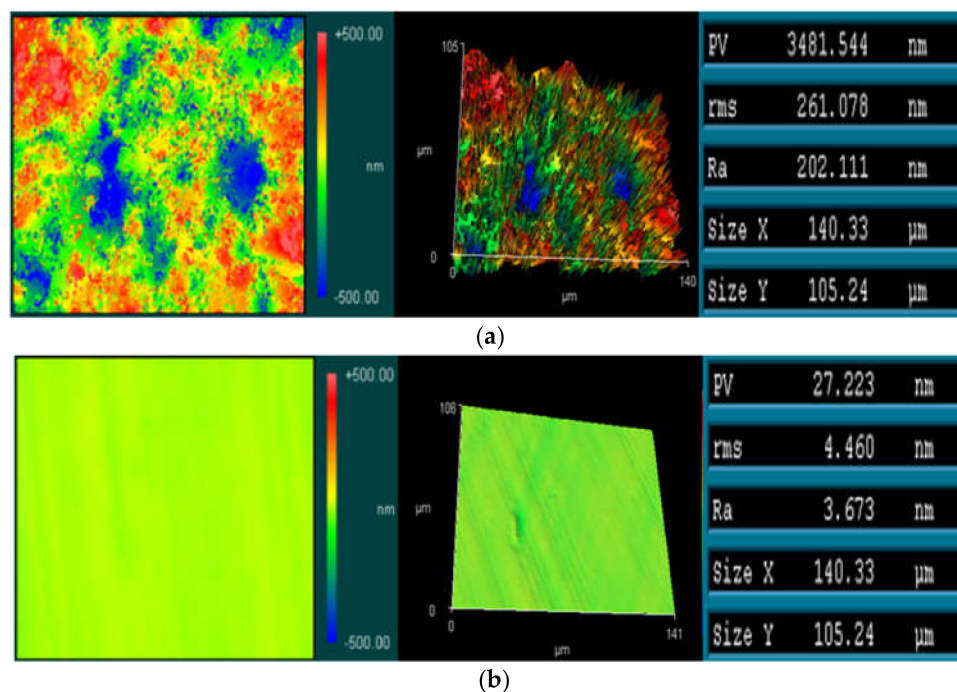


Figure 12. Surface of the workpiece before and after finishing (Load: 10 N, magnetic particles: 330 μm). (a) Before finishing; (b) After finishing.

5. Conclusions

In this work, we propose a new finishing process, which combines the magnetic abrasive finishing process and the fixed abrasive polishing process, analyzed the finishing mechanism of the process, and experimentally verified by finishing alumina ceramics. The main conclusions obtained are as follows:

1. A new finishing process is proposed, which combines the magnetic abrasive finishing process and the fixed abrasive polishing process.
2. Under the experimental conditions, when the average diameter of the magnetic particles is 330 μm and the normal load is 30 N, the best surface quality and the highest finishing efficiency can be obtained.
3. According to the experimental results, the surface roughness of the alumina ceramic plate was improved from 202.11 nm *Ra* to 3.67 nm *Ra* within 30 min.

Author Contributions: Conceptualization, Y.Z. and R.S.; methodology, Y.Z., R.S., O.Y. and H.X.; investigation, Y.Z., R.S., O.Y. and H.X.; writing—original draft preparation, Y.Z., R.S., O.Y. and H.X.; writing—review and editing, Y.Z. and H.X.; supervision, Y.Z.; project administration, Y.Z. and R.S.; funding acquisition, Y.Z. and R.S. All authors have read and agreed to the published version of the manuscript.

Funding: This research was funded by the MEXT Grant-in-Aid for Scientific Research (grant no. JP18K03866) and by The OSAWA Science and Technology Foundation, 2020.

Institutional Review Board Statement: Not applicable.

Informed Consent Statement: Not applicable.

Data Availability Statement: The data presented in this study are available on request from the corresponding author.

Conflicts of Interest: The authors declare no conflict of interest.

References

1. Zou, Y.; Shinmura, T. Development of a new magnetic field assisted deburring technology for inside surface using permanent magnets and magnetic particles: Machining principle and a few deburring characteristics. *J. Jpn. Soc. Abras. Technol.* **2007**, *51*, 94–99. (In Japanese)
2. Yamaguchi, H.; Shinmura, T.; Kobayashi, A. Development of an internal magnetic abrasive finishing process for nonmagnetic complex shaped tubes. *JSME Int. J. Ser. C* **2001**, *44*, 275–281. [[CrossRef](#)]
3. Kala, P.; Pandey, P.M.; Verma, G.C.; Sharma, V. Understanding flexible abrasive brush behavior for double disk magnetic abrasive finishing based on force signature. *J. Manuf. Process.* **2017**, *28*, 442–448. [[CrossRef](#)]
4. Shinmura, T.; Aizawa, T. Study on magnetic abrasive finishing process-development of plane finishing apparatus using a stationary type electromagnet. *Bull. Jpn. Soc. Precis. Eng.* **1989**, *23*, 236–239.
5. Shinmura, T.; Aizawa, T. Development of plane magnetic abrasive finishing apparatus and its finishing performance. (2nd report). Finishing apparatus using a stationary type electromagnet. *J. Jpn. Soc. Precis. Eng.* **1988**, *54*, 928–933. [[CrossRef](#)]
6. Shinmura, T.; Takazawa, K.; Hatano, E.; Matsunaga, M.; Matsuo, T. Study on Magnetic Abrasive Finishing. *CIRP Ann.* **1990**, *39*, 325–328. [[CrossRef](#)]
7. Shinmura, T. Development of Magnetic Abrasive Finishing Apparatus using Vibratory Magnetic Poles and Its Finishing Performance. *JSPE* **1988**, *54*, 2170.
8. Wu, J.; Zou, Y.; Sugiyama, H. Study on ultra-precision magnetic abrasive finishing process using low frequency alternating magnetic field. *J. Magn. Magn. Mater.* **2015**, *386*, 50–59. [[CrossRef](#)]
9. Zou, Y.; Xie, H.; Dong, C.; Wu, J. Study on complex micro surface finishing of alumina ceramic by the magnetic abrasive finishing process using alternating magnetic field. *Int. J. Adv. Manuf. Technol.* **2018**, *97*, 2193–2202. [[CrossRef](#)]
10. Xie, H.; Zou, Y.; Dong, C.; Wu, J. Study on the magnetic abrasive finishing process using alternating magnetic field: Investigation of mechanism and applied to aluminum alloy plate. *Int. J. Adv. Manuf. Technol.* **2019**, *102*, 1509–1520. [[CrossRef](#)]
11. Wang, Y.; Hu, D. Study on the inner surface finishing of tubing by magnetic abrasive finishing. *Int. J. Mach. Tools Manuf.* **2005**, *45*, 43–49. [[CrossRef](#)]
12. Jiao, A.; Zhang, G.; Liu, B.; Liu, W. Study on improving hole quality of 7075 aluminum alloy based on magnetic abrasive finishing. *Adv. Mech. Eng.* **2020**, *12*. [[CrossRef](#)]
13. Vahdati, M.; Vahdati, N. Micromachining of aluminum pipes using magnetic abrasive finishing. *J. Vac. Sci. Technol. B Microelectron. Nanometer Struct. Process. Meas. Phenom.* **2009**, *27*, 1503–1505. [[CrossRef](#)]
14. Gheisari, R.; Ghasemi, A.A.; Jafarkarimi, M.; Mohtaram, S. Experimental studies on the ultra-precision finishing of cylindrical surfaces using magnetorheological finishing process. *Prod. Manuf. Res.* **2014**, *2*, 550–557. [[CrossRef](#)]
15. Yin, S.; Shinmura, T. Vertical vibration-assisted magnetic abrasive finishing and deburring for magnesium alloy. *Int. J. Mach. Tools Manuf.* **2004**, *44*, 1297–1303. [[CrossRef](#)]
16. Yin, S.; Shinmura, T. A comparative study: Polishing characteristics and its mechanisms of three vibration modes in vibration-assisted magnetic abrasive polishing. *Int. J. Mach. Tools Manuf.* **2004**, *44*, 383–390. [[CrossRef](#)]

17. Lin, C.; Yang, L.; Chow, H. Study of magnetic abrasive finishing in free-form surface operations using the Taguchi method. *Int. J. Adv. Manuf. Technol.* **2007**, *34*, 122–130. [[CrossRef](#)]
18. Guo, J.; Jong, H.J.H.; Kang, R.; Guo, D. Novel localized vibration-assisted magnetic abrasive polishing method using loose abrasives for V-groove and Fresnel optics finishing. *Opt. Express* **2018**, *26*, 11608–11619. [[CrossRef](#)]
19. Chen, J.; Zhu, Y.; Wang, J.; Peng, Y.; Yao, J.; Ming, S. Relationship between mechanical properties and processing performance of agglomerated diamond abrasive compared with single diamond abrasive. *Diam. Relat. Mater.* **2019**, *100*, 107595. [[CrossRef](#)]
20. Nguyen, N.Y.; Zhong, Z.W.; Tian, Y.B. Analysis and improvement of the pad wear profile in fixed abrasive polishing. *Int. J. Adv. Manuf. Technol.* **2016**, *85*, 1159–1165. [[CrossRef](#)]
21. Peng, W.; Yao, C.Y.; Lv, X.; Liu, F.Q.; Gao, T.; Yuan, J.L. Experimental Study on New Bonding Materials for Developing Nano-Grinding Plates. *Key Eng. Mater.* **2007**, *329*, 489–494. [[CrossRef](#)]
22. Sato, R. Basic Properties of Fixed Abrasive Polishing by Alumina Abrasive Grain for Si Wafer—Effects of Actual Contact Area and Grain Size-. *Int. J. Autom. Comput.* **2014**, *8*, 592–597. [[CrossRef](#)]
23. Tian, Y.B.; Zhong, Z.W.; Lai, S.T.; Ang, Y.J. Development of fixed abrasive chemical mechanical polishing process for glass disk substrates. *J. Adv. Manuf. Technol.* **2013**, *68*, 993–1000. [[CrossRef](#)]
24. Hu, Z.; Fang, C.; Deng, W.; Zhao, Z.; Lin, Y.; Xu, X. Speed ratio optimization for ceramic lapping with fixed diamond pellets. *J. Adv. Manuf. Technol.* **2017**, *90*, 3159–3169. [[CrossRef](#)]
25. Luo, Q.; Lu, J.; Xu, X. Study on the processing characteristics of SiC and sapphire substrates polished by semi-fixed and fixed abrasive tools. *Tribol. Trans.* **2016**, *104*, 191–203. [[CrossRef](#)]
26. Luo, Q.; Lu, J.; Xu, X. A comparative study on the material removal mechanisms of 6H-SiC polished by semi-fixed and fixed diamond abrasive tools. *Wear* **2016**, *350*, 99–106. [[CrossRef](#)]
27. Huang, S.; Li, X.; Yu, B.; Jiang, Z.; Huang, H. Machining characteristics and mechanism of GO/SiO₂ nanoslurries in fixed abrasive lapping. *J. Mater. Process. Technol.* **2020**, *277*, 116444. [[CrossRef](#)]
28. Zhou, P.; Zhu, N.; Xu, C.; Niu, F.; Li, J.; Zhu, Y. Mechanical removal of SiC by multi-abrasive particles in fixed abrasive polishing using molecular dynamics simulation. *Comput. Mater. Sci.* **2021**, *191*, 110311. [[CrossRef](#)]
29. Cho, B.J.; Kim, H.M.; Manivannan, R.; Moon, D.J.; Park, J.G. On the mechanism of material removal by fixed abrasive lapping of various glass substrates. *Wear* **2013**, *302*, 1334–1339. [[CrossRef](#)]
30. Jiao, F.; Zhao, B. Research on Ultrasonic-Assisted Fixed-Abrasive Lapping Technology for Engineering Ceramics Cylindrical Part. *J. Micro Nanomanuf.* **2017**, *5*, 021001. [[CrossRef](#)]
31. Shinmura, T.; Takazawa, K.; Hatano, E. Study on magnetic abrasive finishing. *Bull. Japan Soc. Precis. Eng.* **1987**, *21*, 139–141. [[CrossRef](#)]
32. Chang, G.; Yan, B.; Hsu, R.T. Study on cylindrical magnetic abrasive finishing using unbonded magnetic abrasives. *Int. J. Mach. Tools Manuf.* **2002**, *42*, 575–583. [[CrossRef](#)]
33. Singh, A.K.; Jha, S.; Pandey, P.M. Design and development of nanofinishing process for 3D surfaces using ball end MR finishing tool. *Int. J. Mach. Tools Manuf.* **2011**, *51*, 142–151. [[CrossRef](#)]
34. Kansal, H.; Singh, A.K.; Grover, V. Magnetorheological nano-finishing of diamagnetic material using permanent magnets tool. *Precis. Eng.* **2018**, *51*, 30–39. [[CrossRef](#)]
35. Yamaguchi, H.; Srivastava, A.K.; Tan, M.A.; Riveros, R.E.; Hashimoto, F. Magnetic abrasive finishing of cutting tools for machining of titanium alloys. *CIRP Ann.* **2012**, *61*, 311–314. [[CrossRef](#)]
36. Natsume, M.; Shinmura, T. Study on the mechanism of plane magnetic abrasive finishing process—Elucidation of normal force characteristics. *Trans. Jpn. Soc. Mech. Eng.* **2008**, *74*, 212–218. (In Japanese) [[CrossRef](#)]
37. Shinmura, T.; Hatano, E.; Takazawa, K. Development of spindle-finish type finishing apparatus and its finishing performance using a magnetic abrasive machining process. *Bull. Jpn. Soc. Precis. Eng.* **1986**, *20*, 79–84. (In Japanese)